Statistical Monitoring of Heteroscedastic Dose-Response Profiles from High-throughput Screening

J. D. Williams, J. B. Birch, W. H. Woodall, and N. M. Ferry

Abstract

In pharmaceutical drug discovery and agricultural crop product discovery, *in vivo* bioassay experiments are used to identify promising compounds for further research. The reproducibility and accuracy of the bioassay is crucial to be able to correctly distinguish between active and inactive compounds. In the case of agricultural product discovery, a replicated dose-response of commercial crop protection products is assayed and used to monitor test quality. The activity of these compounds on the test organisms, the weeds, insects, or fungi, is characterized by a dose-response curve measured from the bioassay. These curves are used to monitor the quality of the bioassays. If undesirable conditions in the bioassay arise, such as equipment failure or problems with the test organisms, then a bioassay monitoring procedure is needed to quickly detect such issues. In this paper we illustrate a proposed nonlinear profile monitoring method to monitor the variability of multiple assays, the adequacy of the dose-response model chosen, and the estimated dose-response curves for aberrant cases in the presence of heteroscedasticity. We illustrate these methods with *in vivo* bioassay data collected over one year from DuPont Crop Protection.

Key Words: Bioassay, Hotelling's T^2 Statistic, Microtiter plates, Multivariate statistical process control, Variance Function.

J. D. Williams is Statistical Leader, GE Global Research, Schenectady, NY 12309 (E-mail: james.williams@research.ge.com). J. B. Birch is Professor, Department of Statistics, Virginia Polytechnic Institute & State University, Blacksburg, VA 24061-0439. W. H. Woodall is Professor, Department of Statistics, Virginia Polytechnic Institute & State University, Blacksburg, VA 24061-0439. N. M. Ferry is Biostatistician, Stine-Haskell Laboratories, DuPont Crop Protection, Newark, DE 19714.

1 Introduction

High throughput screening (HTS) is a common experimental method by which chemical compounds are tested for biological activity (i.e., growth inhibition, growth stimulation, etc.) to test organisms, such as weeds, insects, and fungi (see Delvin (1997) and Janzen (2002)). Agricultural product and pharmaceutical companies frequently use HTS in the discovery phase of chemical and drug development as an efficient method to sift through several thousands of compounds in a short period of time. Paramount to the effectiveness of the HTS is the quality of the testing system in place to identify promising compounds. A testing procedure commonly used is a *bioassay*. Finney (1971, p. 2) described the usefulness of a bioassay in the following way. "Biological assay is a set of techniques relevant to ... the measurement of the potency of any stimulus, physical, chemical or biological, ... by means of the reactions that it produces in living matter. ... Even if the chemical constitution of the material has been determined, there may be little knowledge of the magnitude of the effect which the constituents will produce." Once a compound is identified as being active on a particular test organism, then further in-depth research can be launched to measure its potency, toxicity, and potential environmental risks. However, if a "truly inactive" compound is identified as being active in the HTS and is thereafter advanced to follow-up studies, then valuable time and resources are wasted. This case is referred to as a *false positive*. On the other hand, if a "truly active" compound is not identified in the HTS, then it will be dropped from the potential list of candidate compounds, and there is a potentially large cost for ignoring this promising compound. This case is referred to as a *false negative*. The quality of the bioassay in terms of its accuracy and reproducibility is a significant indicator of the ability of the screen to detect active compounds and eliminate inactive compounds. One expects that the natural variability of the bioassay will cause some false positives and false negatives. However, a high-quality bioassay screen is one that simultaneously minimizes both false positives and false negatives.

Because biological systems have inherent variability, a monitoring procedure of the bioassay is needed to ensure that its quality is maintained. Many factors can influence

the effectiveness of the bioassay, such as pipette accuracy, the health of the test organism being assayed, the growth media, the growth chamber, as well as the measuring device that determines activity. For example, if the test organism becomes weakened, then more test compounds may falsely appear to be active, which may result in increased false positives. On the other hand, if the pipette dispenses too little compound into the microtiter plate, then a "truly active" compound may not be detected, resulting in increased false negatives.

When establishing a control procedure of a product or process, such as a bioassay, a historical dataset (HDS) is required. The HDS consists of data collected from the HTS for a substantial period of time. However, the HDS might contain aberrant bioassay response measurements due to undesirable conditions such as equipment failure or test organism problems. It is desired to remove such out-of-control data from the HDS so that the remaining in-control data can be used to estimate the common-cause variability in the bioassay. Once the in-control process parameters have been estimated, then these estimates can be used in continuous bioassay monitoring. In the case of HTS, an out-of-control signal could indicate that that the bioassay may be unreliable for that sampling period. At that point, further investigation can determine the cause of the out-of-control condition.

Our application is an example of quality profile monitoring, a relatively new area reviewed by Woodall, et al. (2004). The fitted dose-response curves are referred to as profiles. Most of this research thus far has been on linear profiles with a constant variance for the error term. Williams, Woodall, and Birch (2003) proposed nonlinear profile monitoring methodology for the constant variance case, with applications to monitoring the vertical density profile of particle boards manufactured in the forest products industry. In this paper we extend the methodology to the nonlinear profile case with a nonconstant variance. For information on the monitoring of linear profiles, see Kim, et al. (2003) and Mahmoud and Woodall (2004).

2 Bioassay Protocol

One method of determining bioassay quality is to estimate the response of the test organisms in the bioassay to established chemical compounds. For example, in agricultural product development, this is done by employing commercial crop protection products with known properties, hereafter called standards. It is assumed that the commercial compounds are consistent over time. If the activity of a commercial compound is determined to be different from what is expected for the test organism, then the bioassay may be unreliable for that sampling period and is subject to further investigation.

To illustrate our proposed methods we will use an HDS of one year of *in vivo* bioassay results for commercial crop protection products from DuPont Crop Protection. The bioassay protocol that generated this HDS follows a simple four-step procedure. The procedure was the same for both standards and experimental compounds, except that more rates and replicates were used for the standards. However, because the quality of the bioassay is determined using the standards with known properties, we limit the discussion to use of these. In the first step, specified amounts of the test organisms and growth media are pipetted into 96-well microtiter plates of eight rows and twelve columns. Second, the standards are diluted into eight specified doses and pipetted into the microtiter plates, whereupon lids are attached to seal the plates. Four replications per dose of the commercial compound are employed. Third, the plates are stored in a growth chamber for a specified period of time. Fourth, the lids are removed and the response is measured. A spectrophotometer measures the optical density of the remaining test organisms in each well of the microtiter plate. The lower the optical density value, the more activity the compound had on the test organisms. This bioassay of commercial standards is run alongside experimental compounds to assess quality. The DuPont HDS consists of forty-four weekly bioassay tests taken over a one year time period.

We use y_{ijk} to represent the k^{th} response to the j^{th} dose at sampling period i, where $i = 1, \ldots, m$, $j = 1, \ldots, d$, and $k = 1, \ldots, r$. For the DuPont HDS, we have $m = 44$, $d = 8$, and $r = 4$. We cover the profile monitoring methodology based on a balanced HDS

with equal number of replicates per dose and the same dose specifications for all sampling periods. However, because of missing data due to laboratory errors or other reasons, a HDS may not be balanced. The methodology presented here can be extended to the unbalanced case.

Bioassay units with no compound at all are also run alongside experimental compounds as a negative control. These are called *untreated* cases. Optical density readings are taken for these untreated cases to assess the amount of test organisms present at the end of the growth period. The median response of these untreated wells serves as a baseline for the percent control calculations of each experimental unit. We let M_i represent the median response of the untreated specimen at sampling period i. Then, the percent control (PC) of the chemical for the k^{th} replication of the j^{th} dose in sampling period i is calculated as

$$PC_{ijk} = \frac{M_i - y_{ijk}}{M_i}. \tag{1}$$

A plot of PC_{ijk} values for all $m = 44$ weeks for one of the standards from the DuPont HDS is given in Figure 1.

(*Insert Figure 1 about here*)

A dose-response curve must be estimated for each sampling period i using the PC_{ijk} values. Each rate of a standard compound is used as a consistent, reproducible stimulus to detect any variations in the entire bioassay process. When the doses or rates of a standard are summarized together in a dose-response curve, this is a sensitive detector of variations in the bioassay process. For example, if at a sampling period the dose-response curve is quite different than expected, then there is reason to believe that an out-of-control condition has occurred.

The following profile monitoring methodology is divided into two steps: (1) purging the HDS of out-of-control profiles and (2) continuous process monitoring. In the first step, we are concerned with distinguishing between in-control conditions and the presence of assignable causes in the HDS so that in-control model parameters may be estimated for further product or process monitoring in the second step. If out-of-control observations

are included in the estimation of in-control parameters in step one, then the subsequent monitoring procedure will be less effective. Therefore it is imperative that outliers be removed from the HDS and any shifts in the mean response function be identified, so that in-control parameters may be estimated to reflect what would be expected from a stable process. In Sections 3 and 4 we present methods for purging the HDS of out-of-control observations and methods of continuous process monitoring, respectively.

3 Purging the HDS

3.1 Dose-Response Model

For any given chemical compound and test organism, an appropriate dose-response model must be chosen. Subject-matter theory and practical experience often lead to an appropriate model. An ideal model is one that adequately describes the mean response as a function of dose and has parameters with meaningful interpretations.

The shape of the quality profiles can be either linear or nonlinear. Quite often a nonlinear model is needed to adequately describe the relationship between dose and the response in a bioassay. The general form of the nonlinear model used to monitor the response in profile i is

$$y_{ijk} = f(x_{ijk}, \boldsymbol{\beta}_i) + \epsilon_{ijk},\ i = 1, \ldots, m;\ j = 1, \ldots, d;\ k = 1, \ldots, r \tag{2}$$

where y_{ijk} is the k^{th} response from dose x_{ijk}, ϵ_{ijk} is the random error, $\boldsymbol{\beta}_i$ is a $p \times 1$ vector of parameters for profile i, and f is nonlinear in the parameters. The random errors ϵ_{ijk} are assumed to be independent normal random variables with mean zero and variance σ_{ij}^2. Note that the variance of the response is allowed to depend on the dose. Quite often in biological experiments, the variability of the response generally decreases with increasing dose due to the decrease of biological activity. The specific form of σ_{ij}^2 will be modeled in Section 3.2.

A common model used in bioassay experiments to characterize dose-response profiles is

the 4-parameter logistic model, given by

$$y_{ijk} = A_i + \frac{D_i - A_i}{1 + \left(\frac{x_{ijk}}{C_i}\right)^{B_i}} + \epsilon_{ijk}$$

where A_i is the maximal response parameter, D_i is the minimal response parameter, C_i is the ED_{50} parameter (the dose required to elicit 50% response), and B_i is the rate parameter which determines how quickly the response changes from the minimum response to the maximum response (see Ratkowsky (1989) and Schabenberger and Pierce (2002)). When the value of B_i is positive, then the response increases as x_{ijk} increases. When B_i is negative, the response decreases as x_{ijk} increases. We write the vector of parameters in the dose-response model as $\boldsymbol{\beta}_i = (A_i, B_i, C_i, D_i)'$.

3.2 Variance Profile

After the specified dose-response model is chosen to model the mean response, we turn our attention to characterizing the variance of the response as a function of dose. There is a large body of literature on variance function modeling. For a thorough treatment of variance function estimation, see Davidian and Carroll (1987), Carroll and Rupert (1988), and Arbogast and Bedrick (2004). Davidian and Carroll (1987) wrote the general variance function model as

$$\text{Var}(y_{ijk}) = \sigma_{ij}^2 = \sigma_i^2 g(\mathbf{z}_{ij}, \boldsymbol{\beta}_i, \boldsymbol{\theta}_i),$$

where in our case σ_i^2 is a scale parameter for profile i and $g(\cdot)$ is some function of regressor variables $\mathbf{z}_{ij}$, the parameter vector $\boldsymbol{\beta}_i$ from Equation (2), and other parameters $\boldsymbol{\theta}_i$. The variance predictor variables $\mathbf{z}_{ij}$ can be the dose variable, but not necessarily so. The form of $g(\cdot)$ will depend on the specific application.

When there are replications at every dose j, then an unbiased estimator of σ_{ij}^2 can be obtained. The estimator is

$$\hat{\sigma}_{ij}^2 = S_{ij}^2 = \frac{1}{r-1}\sum_{k=1}^{r}(y_{ijk} - \bar{y}_{ij.})^2. \tag{3}$$

If we make the assumption that y_{ijk}, $k = 1, \ldots, r$, are i.i.d. normal random variables (i.e., the r replications within a given dose are independent), then

$$\frac{(r-1)S_{ij}^2}{\sigma_{ij}^2} \sim \chi^2(r-1). \tag{4}$$

One might be tempted to use $1/S_{ij}^2$ as the estimated weights in the subsequent estimation of $\boldsymbol{\beta}$. However, it is well-known that this "connect-the-dots" variance model for small number of replications is hazardous, especially where r is small (see Deaton, Reynolds, and Myers (1983), Davidian and Carroll (1987), and Carroll and Rupert (1988)). Instead, a "smoothed" variance function is preferred.

A useful variance model proposed by Bellio, Jensen, and Seiden (2000) is the so-called "power of x" (POX) model, given by

$$\sigma_{ij}^2 = \sigma_i^2 g(\mathbf{z}_{ij}, \boldsymbol{\beta}_i, \boldsymbol{\theta}_i) = a_{0,i} x_{ij}^{\theta_{1,i}}. \tag{5}$$

Then, as suggested by Aitkin (1987), using the distributional result of Equation (4) we may model S_{ij}^2 using a generalized linear model (GLIM) framework with the natural logarithm link function and gamma errors. Specifically, the GLIM model we use is S_{ij}^2 following a gamma distribution with scale parameter equal to $\frac{r-1}{2}$ and mean function equal to

$$\sigma_{ij}^2 = \exp\{\theta_{0,i} + \theta_{1,i} \log(x_{ij})\}. \tag{6}$$

Note that $\theta_{0,i} = \log(a_{0,i})$. This model is based on the assumption that $\log(S_{ij}^2)$ has a simple linear relationship with $\log(x_{ij})$. Subject-matter theory and experience often give rise to an appropriate variance model. The model given in Equation (6) is illustrated in Section 5 using the DuPont Crop Protection data.

Once the model parameters in Equation (6) are estimated using GLIM techniques, then estimates of σ_{ij}^2 may be obtained. Let $\hat{\theta}_{0,i}$ and $\hat{\theta}_{1,i}$ be the GLIM estimators of $\theta_{0,i}$ and $\theta_{1,i}$, respectively. These estimators have an asymptotic normal distribution, and the estimator of σ_{ij}^2 is

$$(\hat{\sigma}_{ij}^2)^{GLIM} = \exp\{\hat{\theta}_{0,i} + \hat{\theta}_{1,i} \log(x_{ij})\}. \tag{7}$$

We refer to the expression in Equation (7) as the estimated *variance profile* for sampling period i.

In order to check that the estimated variance profiles are in-control, we look for unusual values of $\hat{\theta}_{0,i}$ and $\hat{\theta}_{1,i}$. For example, an extremely large value of $\theta_{0,i}$ could indicate that the overall variability for variance profile i is too large. On the other hand, an out-of-control value of $\theta_{1,i}$ indicates that the rate of increase or decrease of heterogeneity of variance is different for variance profile i. For positive values of $\theta_{1,i}$, the variability increases with x_{ij}, whereas for negative values the variability decreases with x_{ij}.

Since the estimators of $\theta_{0,i}$ and $\theta_{1,i}$ are correlated, it is more appropriate to account for their relationship when testing for unusual values of $\hat{\theta}_{0,i}$ and $\hat{\theta}_{1,i}$. We put $\hat{\theta}_{0,i}$ and $\hat{\theta}_{1,i}$ into a vector as

$$\hat{\boldsymbol{\theta}}_i = \begin{bmatrix} \hat{\theta}_{0,i} \\ \hat{\theta}_{1,i} \end{bmatrix}.$$

One method of identifying multivariate out-of-control variance profiles is use of control charts based on Hotelling's T^2 statistics. The T^2 statistic is a measure of the "distance" between each multivariate observation and the mean observation in a dataset. We write the general form of the T^2 statistic as

$$T_i^2 = \left(\hat{\boldsymbol{\theta}}_i - \hat{\boldsymbol{\mu}}_\theta\right)' \mathbf{S}^{-1} \left(\hat{\boldsymbol{\theta}}_i - \hat{\boldsymbol{\mu}}_\theta\right),$$

where $\hat{\boldsymbol{\mu}}_\theta$ is some estimator of the mean and $\mathbf{S}$ is some estimator of the variance-covariance matrix of the $\hat{\boldsymbol{\theta}}_i$. The T_i^2 statistics are plotted against i in a T^2 *control chart* with a corresponding upper control limit (UCL). Whenever T_i^2 exceeds UCL then an out-of-control signal is observed. Those variance profiles that signaled as out-of-control are subject to investigation and to possibly being removed from the HDS.

A common estimator of the mean is $\bar{\hat{\boldsymbol{\theta}}} = m^{-1} \sum_{i=1}^{m} \hat{\boldsymbol{\theta}}_i$. There are many choices of the estimator $\mathbf{S}$. For a discussion of the various choices of $\mathbf{S}$ and the properties of the corresponding T^2 statistics, see Sullivan and Woodall (1996), Vargas (2003), and Williams, et al. (2006). As shown by Vargas (2003), one choice of $\mathbf{S}$ that is useful for detecting multiple multivariate outliers is one based on the minimum volume ellipsoid (MVE) variance-covariance estimator first proposed by Rousseeuw (1984). Let $\mathbf{S}_{MVE}$ be the MVE estimator

of the variance-covariance matrix and let $\hat{\boldsymbol{\mu}}_\theta^{MVE}$ be the corresponding MVE estimator of the mean vector. Then the T^2 statistics based on $\mathbf{S}_{MVE}$ and $\hat{\boldsymbol{\mu}}_\theta^{MVE}$ are

$$T^2_{MVE,i} = \left(\hat{\boldsymbol{\theta}}_i - \hat{\boldsymbol{\mu}}_\theta^{MVE}\right)' \mathbf{S}^{-1}_{MVE} \left(\hat{\boldsymbol{\theta}}_i - \hat{\boldsymbol{\mu}}_\theta^{MVE}\right). \tag{8}$$

As discussed in Vargas (2003) and Williams, et al. (2006), the distribution of $T^2_{MVE,i}$ is unknown, and hence the UCL must be obtained by simulation.

As a second choice of $\mathbf{S}$, Sullivan and Woodall (1996) and Williams, et al. (2006) recommended use of the variance-covariance matrix based on successive differences of observations. This estimator was shown to be useful for detecting a step or ramp shift in the mean vector, i.e., the value of $\boldsymbol{\theta}$ shifts suddenly or drifts gradually. One example of this is that the overall variability of the bioassay could decrease at some point in the HDS due to deteriorating health of the test organisms, thus causing the value of θ_0 to decrease. To obtain the estimator, we define $\mathbf{v}_i = \hat{\boldsymbol{\theta}}_{i+1} - \hat{\boldsymbol{\theta}}_i$ for $i = 1, \ldots, m-1$ and stack the transpose of these $m-1$ difference vectors into the $(m-1) \times 2$ matrix $\mathbf{V}$ as

$$\mathbf{V} = \begin{bmatrix} \mathbf{v}_1' \\ \mathbf{v}_2' \\ \vdots \\ \mathbf{v}_{m-1}' \end{bmatrix}.$$

The estimator of the variance-covariance matrix is then

$$\mathbf{S}_D = \frac{\mathbf{V}'\mathbf{V}}{2(m-1)}.$$

This estimator is analogous to the univariate moving range estimator of the variance in the construction of an X-chart. We write the corresponding T^2 statistics based on $\mathbf{S}_D$ as

$$T^2_{D,i} = \left(\hat{\boldsymbol{\theta}}_i - \bar{\hat{\boldsymbol{\theta}}}\right)' \mathbf{S}_D^{-1} \left(\hat{\boldsymbol{\theta}}_i - \bar{\hat{\boldsymbol{\theta}}}\right). \tag{9}$$

Unfortunately, the exact distribution of the $T^2_{D,i}$ statistics is unknown. However, as shown by Williams, et al. (2006), the asymptotic distribution of $T^2_{D,i}$ is a good approximate distribution whenever the number of samples m in the HDS is greater than $p^2 + 3p$, where p is the number of parameters being estimated in $\hat{\boldsymbol{\theta}}_i$. In this case the asymptotic distribution of $T^2_{D,i}$ is $\chi^2(p)$, for all $i = 1, \ldots, m$. For smaller m, an approximate distribution based on

the beta distribution could be used. The approximate distribution is given in Williams, et al. (2006). For large m the UCL is calculated as

$$UCL_{T^2} = \chi^2(1-\alpha_I, p),$$

where $\chi^2(q,p)$ is the q^{th} quantile from a χ^2 distribution with p degrees of freedom and α_I is an appropriately chosen nominal false alarm probability. When examining each profile for unacceptable variance, we use a Bonferroni correction to protect against inflating the probability of a false alarm. Although other corrections are possible, the Bonferroni correction is the most conservative. We let α_I be the probability of a false alarm for any individual T^2 statistic. Then the overall probability of a false alarm for a sample of m profiles is approximately $\alpha_{overall} = 1-(1-\alpha_I)^m$. Thus, for a given overall probability of a false alarm, we use

$$\alpha_I = 1-(1-\alpha_{overall})^{1/m} \tag{10}$$

in calculation of UCLs. Common choices of $\alpha_{overall}$ are 0.05 and 0.01.

For purging the HDS of out-of-control observations, we recommend use of two T^2 control charts, one based on $T^2_{MVE,i}$ statistics and one based on $T^2_{D,i}$ statistics, with their associated UCLs. Those variance profiles that are determined to be out-of-control are investigated and potentially removed from the HDS. We let m' represent the number of remaining profiles in the HDS. With the m' remaining in-control variance profiles we move our attention to analyzing the estimated mean profiles of the HDS.

3.3 Mean Profile

With the variance function estimates for the in-control variance profiles, we can calculate estimates of $\boldsymbol{\beta}_i$ for the remaining profiles in the HDS using $w_{ij} = (\hat{\sigma}_{ij}^{-2})^{GLIM}$ as weights. This is done via standard weighted nonlinear least squares (WNLS) methods using the dose-response model chosen in Section 3.1. As a first step, initial estimates for all model parameters need to be selected. It is very important to specify good starting values for the model estimation. In finding good starting values, we recommend using as wide a grid

search as time and computing resources allow. This is necessary since m' profiles are being fit using the same dose-response model. Inadequate starting values can lead to poor fits. It may also be necessary to impose boundary constraints on the parameters if the estimation algorithm fails to converge.

We then seek to identify out-of-control mean profiles. Two specific forms of out-of-control conditions we seek to identify are (1) changes in the functional from of the model and (2) unusual values of $\hat{\boldsymbol{\beta}}_i$. The first will be evaluated in terms of lack-of-fit (LOF) methods. The second will be addressed in terms of a T^2 control chart.

3.3.1 Lack-of-Fit

The most severe type of out-of-control profile is one where the underlying dose-response model is different from the hypothesized model. This may be due to a number of causes, including hormesis (spontaneous biological activity), biological variability, or even human error. Often chemical and drug companies will produce their own test organisms in-house for use in bioassay experimentation. If the susceptibility of the test organisms changes over time then the dose-response model may no longer adequately describe the mean response as a function of dose.

Constructing a true LOF test for the case of nonlinear regression with heteroscedastic errors is a topic of current research. Bedrick (2000) and Arbogast and Bedrick (2004) proposed goodness-of-fit tests for the linear regression model with heterogenous variances for the non-replicated case, but this does not directly apply to replicated dose-response data as is often the case in bioassay experiments.

One approach is to employ classical LOF methodology, substituting sums of squares with weighted sums of squares, where the weights are equal to w_{ij}. The LOF statistic compares the error sum of squares of a saturated model, sometimes called the means or full model, to the error sum of squares of the specified regression model. Specifically, the weighted sum of squared errors for the saturated model is

$$WSSE_i^{full} = \sum_{j=1}^{d} \sum_{k=1}^{r} w_{ij}(y_{ijk} - \bar{y}_{ij.})^2,$$

where $\bar{y}_{ij\cdot} = r^{-1}\sum_{k=1}^{r} y_{ijk}$ is the mean of the r replications at dose j in profile i. Further, we let $\hat{y}_{ijk}$ represent the estimated response for dose j and replication k of profile i, obtained via WNLS. Then the weighted sum of squared errors for the nonlinear regression model is given by

$$WSSE_i^{reg} = \sum_{j=1}^{d}\sum_{k=1}^{r} w_{ij}(y_{ijk} - \hat{y}_{ijk})^2.$$

The lack-of-fit statistic compares the nonlinear model fit to the saturated model. Using a small adjustment to the deviance test for lack-of-fit for the replicated normal data with heteroscedasticity, we propose the lack-of-fit statistic for profile i as

$$LOF_i = \frac{(WSSE_i^{reg} - WSSE_i^{full})/df^{LOF}}{WSSE_i^{full}/df^{full}}, \tag{11}$$

where $df^{LOF} = d-p$ represents the degrees of freedom for the lack-of-fit and $df^{full} = d(r-1)$ represents the degrees of freedom of the full model. As given in Neill (1988), the LOF_i statistic for the nonlinear regression case with homogeneous variance approximately follows an $\mathcal{F}$ distribution with df^{LOF} and df^{full} numerator and denominator degrees of freedom, respectively. However, due to the heteroscedasticity typically present dose-response data, the distribution of this statistic no longer follows the $\mathcal{F}$-distribution, but may be approximated very well by an $\mathcal{F}$-distribution.

To assess lack-of-fit for profile i, we plot all LOF_i statistics versus i in a *lack-of-fit chart*. The UCL for the lack-of-fit chart is given by

$$UCL_{LOF} = \mathcal{F}(1-\alpha_I, df^{LOF}, df^{full}), \tag{12}$$

where $\mathcal{F}(q, df_1, df_2)$ is the q^{th} quantile from an $\mathcal{F}$ distribution with df_1 and df_2 numerator and denominator degrees of freedom, respectively. Whenever LOF_i exceeds UCL_{LOF}, the proposed dose-response model is determined to be inadequate for profile i. Those profiles that exhibit lack-of-fit are subject to being removed from the HDS. We let m'' represent the number of remaining in-control profiles, where $m'' \leq m' \leq m$.

3.3.2 Identifying Abnormal Mean Profiles

For those mean profiles that are are not determined to have significant lack-of-fit, we seek to identify and remove unusual values of $\hat{\boldsymbol{\beta}}_i$ from the HDS. Because nonlinear regression parameter estimators are correlated, we must account for their correlations in the analysis. As in the case of $\hat{\boldsymbol{\theta}}_i$ of Section 3.2, we calculate T^2 statistics to identify both multivariate outliers and step or ramp shifts in the vector $\boldsymbol{\beta}$. Specifically, let $\hat{\boldsymbol{\mu}}_{\beta}^{MVE}$ and $\mathbf{S}_{\beta,MVE}$ be the MVE estimators of the mean vector and variance-covariance matrix of the $\hat{\boldsymbol{\beta}}_i$ vectors. Then the corresponding T^2 statistics based on the MVE estimators are defined as

$$T^2_{MVE,i} = \left(\hat{\boldsymbol{\beta}}_i - \hat{\boldsymbol{\mu}}_{\boldsymbol{\beta}}^{MVE}\right)' \mathbf{S}^{-1}_{\beta,MVE} \left(\hat{\boldsymbol{\beta}}_i - \hat{\boldsymbol{\mu}}_{\beta}^{MVE}\right). \tag{13}$$

Similarly, let $\mathbf{S}_{\beta,D}$ be the variance-covariance matrix estimator based on successive differences. Then the T^2 statistics based on the successive differences variance-covariance matrix estimator are defined as

$$T^2_{MVE,i} = \left(\hat{\boldsymbol{\beta}}_i - \bar{\hat{\boldsymbol{\beta}}}\right)' \mathbf{S}^{-1}_{\beta,D} \left(\hat{\boldsymbol{\beta}}_i - \bar{\hat{\boldsymbol{\beta}}}\right), \tag{14}$$

where $\bar{\hat{\boldsymbol{\beta}}} = \frac{1}{m''}\sum_{i=1}^{m''} \hat{\boldsymbol{\beta}}_i$. The UCLs for the two T^2 charts are defined as in Section 3.2.

Using the T^2 charts and the associated UCLs we investigate and possibly remove the out-of-control profiles from the HDS, and the remaining profiles in the HDS are presumed to represent in-control profiles. Let $m^\star$ represent the number of in-control profiles in the HDS. Then, the last step in this phase of the analysis is to estimate the in-control mean vector $\boldsymbol{\mu}_\beta$ and covariance matrix $\boldsymbol{\Sigma}_\beta$ for use in continuous process monitoring, as discussed in Section 4. Using the remaining $m^\star$ in-control profiles from the HDS, the final estimate of $\boldsymbol{\mu}_\beta$ is calculated as

$$\hat{\boldsymbol{\mu}}_\beta = \bar{\hat{\boldsymbol{\beta}}} = \frac{1}{m^\star}\sum_{i=1}^{m^\star} \hat{\boldsymbol{\beta}}_i \tag{15}$$

and the final estimate of $\boldsymbol{\Sigma}_\beta$ is

$$\hat{\boldsymbol{\Sigma}}_\beta = \frac{1}{m^\star - 1}\sum_{i=1}^{m^\star} \left(\hat{\boldsymbol{\beta}}_i - \bar{\hat{\boldsymbol{\beta}}}\right)\left(\hat{\boldsymbol{\beta}}_i - \bar{\hat{\boldsymbol{\beta}}}\right)'. \tag{16}$$

In addition, we estimate the in-control values of $\boldsymbol{\theta}$ from the variance profile model of Section 3.2. Using the $m^\star$ in-control profiles from the HDS, we calculate the moment

estimators

$$\hat{\boldsymbol{\mu}}_\theta = \frac{1}{m^\star} \sum_{i=1}^{m^\star} \hat{\boldsymbol{\theta}}_i \tag{17}$$

and

$$\hat{\boldsymbol{\Sigma}}_\theta = \frac{1}{m^\star - 1} \sum_{i=1}^{m^\star} \left(\hat{\boldsymbol{\theta}}_i - \hat{\boldsymbol{\mu}}_\theta \right) \left(\hat{\boldsymbol{\theta}}_i - \hat{\boldsymbol{\mu}}_\theta \right)'. \tag{18}$$

4 Continuous Process Monitoring

Once the in-control mean and variance profiles are obtained, we construct control charts for ongoing monitoring of the bioassay. The bioassay experiment is conducted at time t ($t = 1, \dots$), and the mean profile and the variance profile model of Sections 3.1 and 3.2, respectively, are estimated. We seek to quickly detect any out-of-control profiles, which may indicate that the bioassay is unreliable.

The charts used in this phase of the analysis are similar to the charts used in the previous phase. The three charts used are the T^2 chart for the variance profile, the lack-of-fit chart, and a T^2 chart for the mean profile. However, instead of using α_I of Equation (10), we choose an appropriate probability of a false alarm α_{II} in continuous process monitoring. A common choice of α_{II} is $\alpha_{II} = 0.001$.

Whenever new equipment is introduced to the bioassay or there is some other reason to believe that the in-control mean profile has changed, then a new HDS should be collected and the methods of the previous phase repeated. This is especially the case for biological processes, which are very sensitive to changes in environmental conditions.

4.1 Variance Profile Monitoring

To monitor the variance profile collected at time t, we employ the variance profile model of Section 3.2 to estimate the value of $\boldsymbol{\theta}$ from the bioassay conducted at time t. We then use the estimated mean vector and variance-covariance matrix of $\hat{\boldsymbol{\theta}}$, given in Equations (17) and (18), to construct a T^2 control chart. The $T_t^2,\ t = 1, 2, 3, \dots$, statistics are calculated as

$$T_t^2 = \left(\hat{\boldsymbol{\theta}}_t - \hat{\boldsymbol{\mu}}_\theta \right)' \hat{\boldsymbol{\Sigma}}_\theta^{-1} \left(\hat{\boldsymbol{\theta}}_t - \hat{\boldsymbol{\mu}}_\theta \right).$$

The UCL for this chart is given by

$$UCL_{T^2_\theta} = \frac{2(m^\star+1)(m^\star-1)}{m^\star(m^\star-2)}\mathcal{F}(1-\alpha_{II}, p, m^\star-2)$$

(Mason, Chou, and Young, 2001). Whenever $T_t^2 > UCL_{T^2_\theta}$ then the chart signals, and hence profile t is subject to further investigation.

4.2 The Lack-of-Fit Control Chart

Lack-of-fit can be assessed at time t using methods analogous to those in Section 3.3.1. From the bioassay data obtained at time t, we calculate the LOF statistic as

$$LOF_t = \frac{(WSSE_t^{reg} - WSSE_t^{full})/df_t^{LOF}}{WSSE_t^{full}/df^{full}}.$$

As mentioned in Section 3.3.1, the LOF_t statistic follows an approximate $\mathcal{F}$ distribution with df^{LOF} and df^{full} numerator and denominator degrees of freedom, respectively. We plot all LOF_t statistics by t in a lack-of-fit chart. The associated UCL is given by

$$UCL_{LOF} = \mathcal{F}(1-\alpha_{II}, df^{LOF}, df^{full}).$$

Whenever LOF_t exceeds UCL_{LOF}, then it is determined that the proposed dose-response model has changed for profile t, and is subject to further investigation.

4.3 The T^2 Control Chart

The third control chart is the T^2 chart, useful for quickly detecting profiles with unusual estimated parameter values. The T^2 statistic for profile t uses the estimates of $\boldsymbol{\mu}_\beta$ and $\boldsymbol{\Sigma}_\beta$ of Equations (15) and (16), respectively. The T^2 statistic is given by

$$T_t^2 = \left(\hat{\boldsymbol{\beta}}_t - \hat{\boldsymbol{\mu}}_\beta\right)' \hat{\boldsymbol{\Sigma}}_\beta^{-1} \left(\hat{\boldsymbol{\beta}}_t - \hat{\boldsymbol{\mu}}_\beta\right).$$

An approximate distribution of T_t^2 is given by

$$T_t^2 \frac{m^\star(m^\star-p)}{p(m^\star+1)(m^\star-1)} \sim \mathcal{F}(p, m^\star-p),$$

where p is the dimension of $\hat{\boldsymbol{\beta}}$ (Mason, Chou, and Young, 2001). The UCL is then calculated as

$$UCL_{T^2} = \frac{p(m^\star + 1)(m^\star - 1)}{m^\star(m^\star - p)} \mathcal{F}(1 - \alpha_{II}, p, m^\star - p).$$

Whenever T_t^2 exceeds UCL_{T^2} then profile t is declared to be out-of-control, and is subject to further investigation.

5 Example

To illustrate the profile monitoring methods of Section 3, we analyze the HDS from DuPont Crop Protection given in Figure 1 . The data consists of forty-four weeks ($m = 44$) of *in vivo* bioassay results for standards (commercial crop protection products) run alongside experimental compounds over a one-year time period. The bioassay procedure described in Section 2 was employed using a commercial crop protection product and a test organism. Because of the proprietary nature of the bioassay, the commercial compound and test organism used are undisclosed.

The commercial compound was diluted to eight doses (0.003, 0.009, 0.028, 0.084, 0.25, 0.76, 2.27, and 6.8) and replicated four times at each dose ($r = 4$) in 96-well microtiter plates for each sampling period i. A spectrophotometer measured the optical density (OD) of the plant organism after the inoculation period. Both treated and untreated wells were measured for growth inhibition. The PC_{ijk} values were calculated using the median OD (M_i) from 96 replications of untreated wells, as given in Equation (1).

The data plotted in Figure 1 indicate the presence of heterogeneity of variance across the eight doses within each profile. The dominate pattern seen is that the sample variance based on four replicates at each dose appears to be larger at the smaller doses than at the larger doses. There are several exceptions to this as seen in the plots for weeks 6, 22, 24, 26, and 45. Based on subject-matter theory of the biological process, our proposed variance model is the POX model given in Equation (5). We employed Equation (3) to calculate S_{ij}^2 for $i = 1, \ldots, 44$ and $j = 1, \ldots, 4$, used the distributional properties of the S_{ij}^2 statistics

given in Equation (4), and employed a GLIM model from Equation (6). Using this model we obtained values of the estimators $\hat{\theta}_{0,i}$ and $\hat{\theta}_{1,i}$ for all 44 weeks of the DuPont data.

To graphically visualize the goodness-of-fit of this model, we plot the $\log(S_{ij}^2)$ versus the logarithm of dose and superimpose the logarithm of the predicted values of the variance from Equation (7), given by $\log\left((\hat{\sigma}_{ij}^2)^{GLIM}\right)$. The plot is given in Figure 2. A plot of the 44 variance profiles overlaid in one graph is given in Figure 3.

(*Insert Figures 2 and 3 about here*)

To check for unusual variance profiles, we calculated $T_{MVE,i}^2$ and $T_{D,i}^2$ statistics based on the values of $\hat{\boldsymbol{\theta}}_i$, as given in Equations (8) and (9), respectively. We chose $\alpha_{overall} = 0.05$, which corresponds to $\alpha = 0.001165$, as given in Equation (10). The UCL for the chart based on $T_{D,i}^2$ is 13.51 and the UCL for the chart based on the MVE (obtained via simulation) is approximately 23. The two charts are given in Figure 4.

(*Insert Figure 4 about here*)

The T^2 chart based on the $T_{D,i}^2$ statistic does not signal, whereas observations 6, 20, 22, 24, 26, and 45 produced a signal in the chart based on $T_{MVE,i}^2$. Recall that the T^2 chart based on $T_{D,i}^2$ statistics is not as powerful in detecting multivariate outliers as the chart based on the $T_{MVE,i}^2$ statistics. The observations that signal are extreme in both $\theta_{0,i}$ and $\theta_{1,i}$. In Figure 5 we plot the forty-four ordered pairs $\hat{\theta}_{0,i}$ and $\hat{\theta}_{1,i}$. The six weeks that produced the signal are extreme in both $\theta_{0,i}$ and $\theta_{1,i}$. All are associated with variance profiles with a positive slope value $\hat{\theta}_{1,i}$ Hence, these observations are removed from the HDS, resulting in $m' = 38$.

(*Insert Figure 5 about here*)

Now we use WNLS to estimate the mean profiles, where the estimated weights are $(\hat{\sigma}_{ij}^{-2})^{GLIM}$ from Equation (7). For completeness, we illustrate the estimated mean profiles for all forty-four weeks in Figure 6.

(*Insert Figure 6 about here*)

To check for appropriateness of the mean profile model, we calculated the lack-of-fit statistic of Equation (11) based on the weighted sums of squares. From Equation (12) the approximate UCL associated with the chart is 6.26, and the chart is given in Figure 7.

(*Insert Figure 7 about here*)

Although weeks 21, 30, 32, and 33 produced a signal, only observations 21 and 32 were removed from the HDS. Weeks 30 and 33 exhibit only marginal lack-of-fit. This leaves $m'' = 36$ profiles remaining in the HDS.

Next we checked for unusual values of estimated parameters using a T^2 chart based on the $T^2_{MVE,i}$ and $T^2_{D,i}$ statistics, as given in Equations (13) and (14), respectively. The UCLs associated with the charts are 38 and 17.68, respectively. The charts are given in Figure 8.

(*Insert Figure 8 about here*)

Weeks 13, 34, and 48 produced a signal in the T^2 chart based on $T^2_{MVE,i}$, and observations 13 and 34 produced a signal in the chart based on $T^2_{D,i}$. All three of these weeks were removed from the HDS. Subsequently, a second T^2 chart was created to further check for out-of-control profiles after removing these weeks. The new UCLs for the two charts are 40 and 17.49, respectively. The charts are given in Figure 9.

(*Insert Figure 9 about here*)

Week 46 was identified as being out-of-control and was removed from the HDS. The remaining weeks were presumed to be in-control. A plot of the in-control estimated mean profiles is given in Figure 10.

(*Insert Figure 10 about here*)

The remaining $m^\star = 32$ profiles are now used to estimate the in-control mean vector and variance-covariance matrix of $\hat{\boldsymbol{\theta}}_i$ and the in-control mean vector and variance-covariance

matrix of $\hat{\boldsymbol{\beta}}_i$ for future process monitoring. From Equations (17) and (18) the estimates for the the variance profile are calculated as

$$\hat{\boldsymbol{\mu}}_\theta = \begin{bmatrix} -9.326028 \\ -0.765682 \end{bmatrix}$$

and

$$\hat{\boldsymbol{\Sigma}}_\theta = \begin{bmatrix} 2.4730289 & 0.5147257 \\ 0.5147257 & 0.1396993 \end{bmatrix}.$$

From Equations (15) and (16) the estimates for the the mean profile are calculated as

$$\hat{\boldsymbol{\mu}}_\beta = \begin{bmatrix} 0.8959855 \\ 2.3857821 \\ 0.0608633 \\ 0.4227484 \end{bmatrix}$$

and

$$\hat{\boldsymbol{\Sigma}}_\beta = \begin{bmatrix} 0.0001282 & -0.000134 & -0.000055 & 0.0000786 \\ -0.000134 & 0.4280911 & 0.0067914 & 0.0120498 \\ -0.000055 & 0.0067914 & 0.0004831 & 0.0002597 \\ 0.0000786 & 0.0120498 & 0.0002597 & 0.0017581 \end{bmatrix}.$$

6 Discussion

In the DuPont dataset, there are a number of mean and variance profiles that have outliers, and these outliers can have an undue influence on the parameter estimates. The estimate of the variance profile is particularly influenced by outliers. For example, in Figure 1, we see that in weeks 6 and 45 there are outliers, and the corresponding variance and mean profile parameter estimates are slightly distorted, as seen in Figures 2 and 6. An alternative approach would be to use outlier-robust methods to model both the mean and variance profiles for purging the HDS of out-of-control profiles. Since the goal is to obtain an in-control estimate of the mean vector and the covariance matrix of the parameter estimators, then it makes sense to use outlier-robust methods to down weight the influence of outliers. The subsequent in-control mean vector and covariance matrix can then be calculated from the robust estimates. Use of such robust nonlinear modeling is a topic for further research.

In Sections 3.2 and 3.3.2 we recommended use of two T^2 control charts, one based on $T^2_{MVE,i}$ values and one based on $T^2_{D,i}$ values. The former chart is useful for detecting the presence of multiple multivariate outliers and the latter is useful for detecting the presence

of a sustained shift in the mean vector. However, since the $T^2_{MVE,i}$ and $T^2_{D,i}$ statistics are not independent then using both charts together inflates the probability of a false alarm. In order to achieve a desired false alarm rate, the two control limits should both presumably increase in order to control for multiple testing. The exact control limits needed for this control chart combination is a topic for further research.

The methods we have proposed here are based on parametric models. One appeal of a parametric approach in monitoring the dose-response quality profiles is the interpretability of the model parameters. Although a nonparametric approach may be able to fit unusual dose-response profile shapes more readily, the interpretation is not as clear. Further, there is no guarantee that the nonparametric fit will conform to the underlying biological model. Hence we recommend use of parametric modeling for continuous dose-response profile monitoring.

7 Conclusion

We have introduced continuous process monitoring methodology for the case of heteroscedastic dose-response profiles. The analysis began with purging the HDS of out-of-control mean and variance profiles. Out-of-control profiles are identified based on control charts to detect the presence of special causes in (1) the variance profile, (2) the functional form of the mean profile, and (3) the mean profile. Those profiles that produced a signal in the charts were subject to investigation and possible removal from the HDS. The remaining in-control observations were subsequently used to estimate in-control mean and variance profile model parameters for continuous process monitoring.

First, we proposed use of a variance function model to aid in monitoring the heteroscedasticity often present in bioassay experimentation. The HDS was purged of out-of-control variance profiles through use of T^2 control charts based on variance profile parameter estimates.

Second, we proposed use of a lack-of-fit chart to detect the presence of a change in the functional form of the mean profiles of the HDS. The chart is based on the traditional

lack-of-fit $\mathcal{F}$ statistic with the modification that sums of squares are replaced with weighted sums of squares, where the weights are calculated based on the estimated variance profiles.

Third, we proposed use of T^2 control charts based on estimated parameter values of the mean profiles in order to check for aberrant mean profiles. The mean profile estimates were based on a WNLS estimation of the dose-response profiles, where the weights were obtained from the estimated variance profiles.

To illustrate the proposed methods, we employed an HDS from DuPont Crop Protection consisting of forty-four weekly dose-response results for standards run alongside experimental compounds from their high-throughput screening. Twelve weeks produced signals in the control charts, were subsequently deemed as out-of-control, and removed from the HDS. In-control mean and variance profile parameters were estimated from the remaining thirty-two weeks for continuous process monitoring.

In HTS, replication for experimental compounds is often limited. However, a replicated dose-response of standards can be used to monitor effectively the quality of the bioassay used in screening.

References

Aitkin, M. (1987), "Modelling Variance Heterogeneity in Normal Regression using GLIM," *Applied Statistics*, 36, pp. 332-339.

Arbogast, P. G., and Bedrick, E. J. (2004), "Model-Checking Techniques for Linear Models with Parametric Variance Functions," *Technometrics*, 46, pp. 404-410.

Bedrick, E. J. (2000), "Checking for Lack of Fit in Linear Models With Parametric Variance Functions," *Technometrics*, 42, pp. 227-236.

Bellio, R., Jensen, J. E., and Seiden, P. (2000), "Applications of Likelihood Asymptotics for Nonlinear Regression in Herbicide Bioassays," *Biometrics*, 56, pp. 1204-1212.

Carroll, R. J., and Ruppert, D. (1988), *Transformation and Weighting in Regression*, New York: Chapman and Hall.

Davidian, M., and Carroll, R. J. (1987), "Variance Function Estimation," *Journal of the American Statistical Association* 82, pp. 1079-1091.

Deaton, M. L., Reynolds, M. R., Jr., and Myers, R. H. (1983), "Estimation and Hypothesis Testing in Regression in the Presence of Nonhomogeneous Error Variances," *Communications in Statistics, Part B – Simulation and Computation*, 12, pp. 45-66.

Delvin, J. P. (1997), *High Throughput Screening: The Discovery of Bioactive Substances*, New York: Marcel Dekker.

Finney, D. J. (1971), *Probit Analysis*, London: Cambridge University Press.

Janzen, W. P. (2002), *High Throughput Screening: Methods and Protocols*, Totowa, New Jersey: Humana Press.

Kim, K., Mahmoud, M. A., and Woodall, W. H. (2003), "On the Monitoring of Linear Profiles," *Journal of Quality Technology*, 35, pp. 317-328.

Mahmoud, M. A. and Woodall, W. H. (2004), "Phase I Analysis of Linear Profiles with Calibration Applications". *Technometrics*, 46, pp. 380-391.

Mason, R. L., Chou, Y. -M., and Young, J. C. (2001), "Applying Hotelling's T^2 Statistic to Batch Processes". *Journal of Quality Technology* 33, pp. 466-479.

Neill, J. W. (1988), "Testing For Lack-of-Fit in Nonlinear Regression". *The Annals of Statistics* 16, pp. 733-740.

Ratkowsky, D. A. (1989), *Handbook of Nonlinear Regression Models*, New York: Marcel Dekker.

Rousseeuw, P. J. (1984), "Least Median of Squares Regression," *Journal of the American Statistical Association*, 79, pp. 871-880.

Schabenberger, O., and Pierce F. J. (2002), *Contemporary Statistics for the Plant and Soil Sciences*, Boca Raton, Florida: CRC Press.

Sullivan, J. H. and Woodall, W. H. (1996), "A Comparison of Multivariate Control Charts for Individual Observations". *Journal of Quality Technology* 28, pp. 398-408.

Vargas J. A. (2003), "Robust Estimation in Multivariate Control Charts for Individual Observations". *Journal of Quality Technology* 35, pp. 367-376.

Williams, J. D., Woodall, W. H., Birch, J. B. (2003), "Phase I Analysis of Nonlinear Product and Process Quality Profiles," Technical Report No. 03-5, Department of Statistics, Virginia Polytechnic Institute and State University.

Williams, J. D., Woodall, W. H., Birch, J. B., and Sullivan, J. H. (2006), "On the Distribution of T^2 Statistics Based on Successive Differences," *Journal of Quality Technology*, In print.

Woodall, W. H., Spitzner, D. J., Montgomery, D. C., and Gupta, S. (2004), "Using Control Charts to Monitor Process and Product Quality Profiles". *Journal of Quality Technology* 36, pp. 309-320.

Figure 1: DuPont Dose-Response Data for $m = 44$ weeks

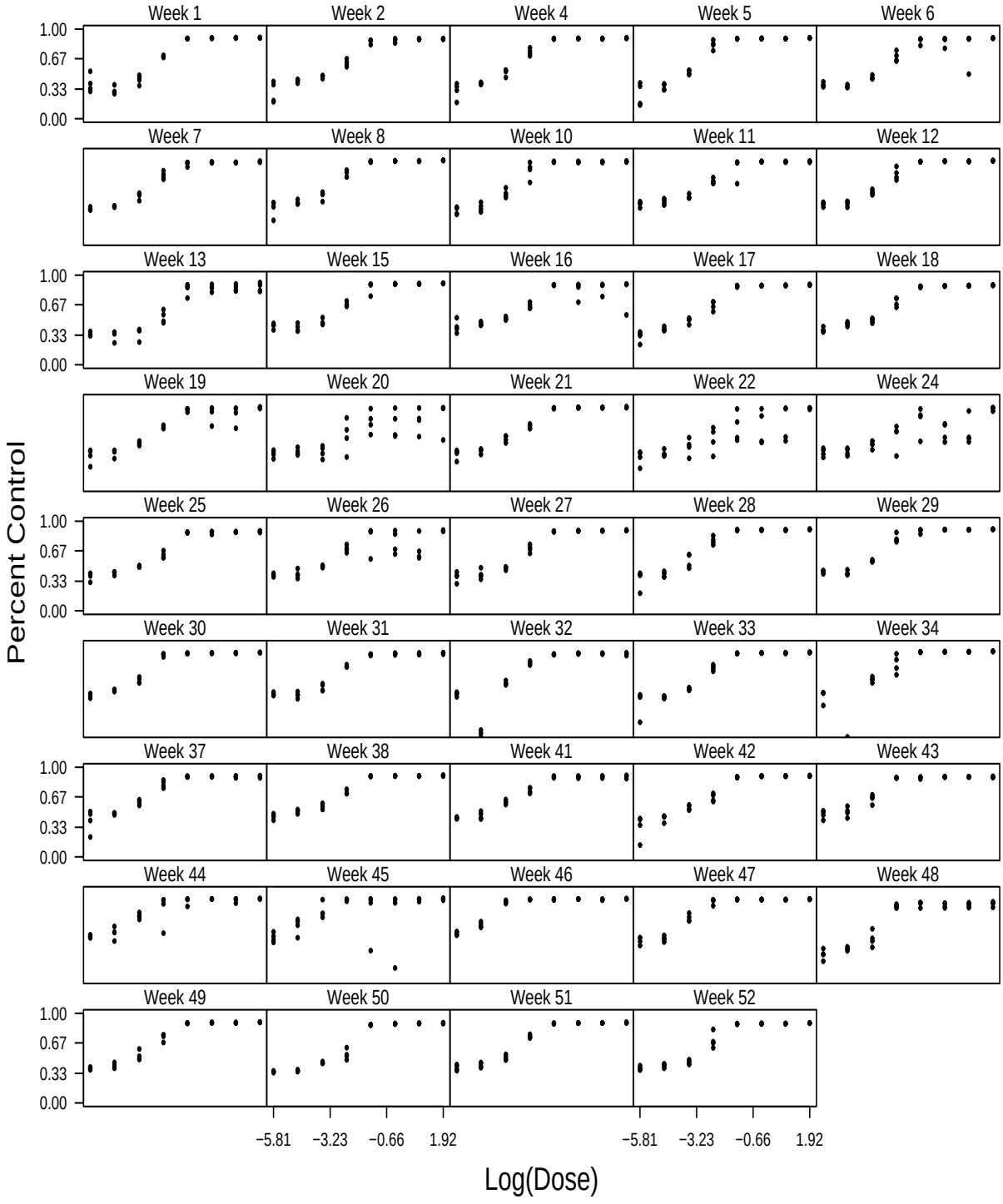

Figure 2: Estimated variance profiles for all 44 weeks.

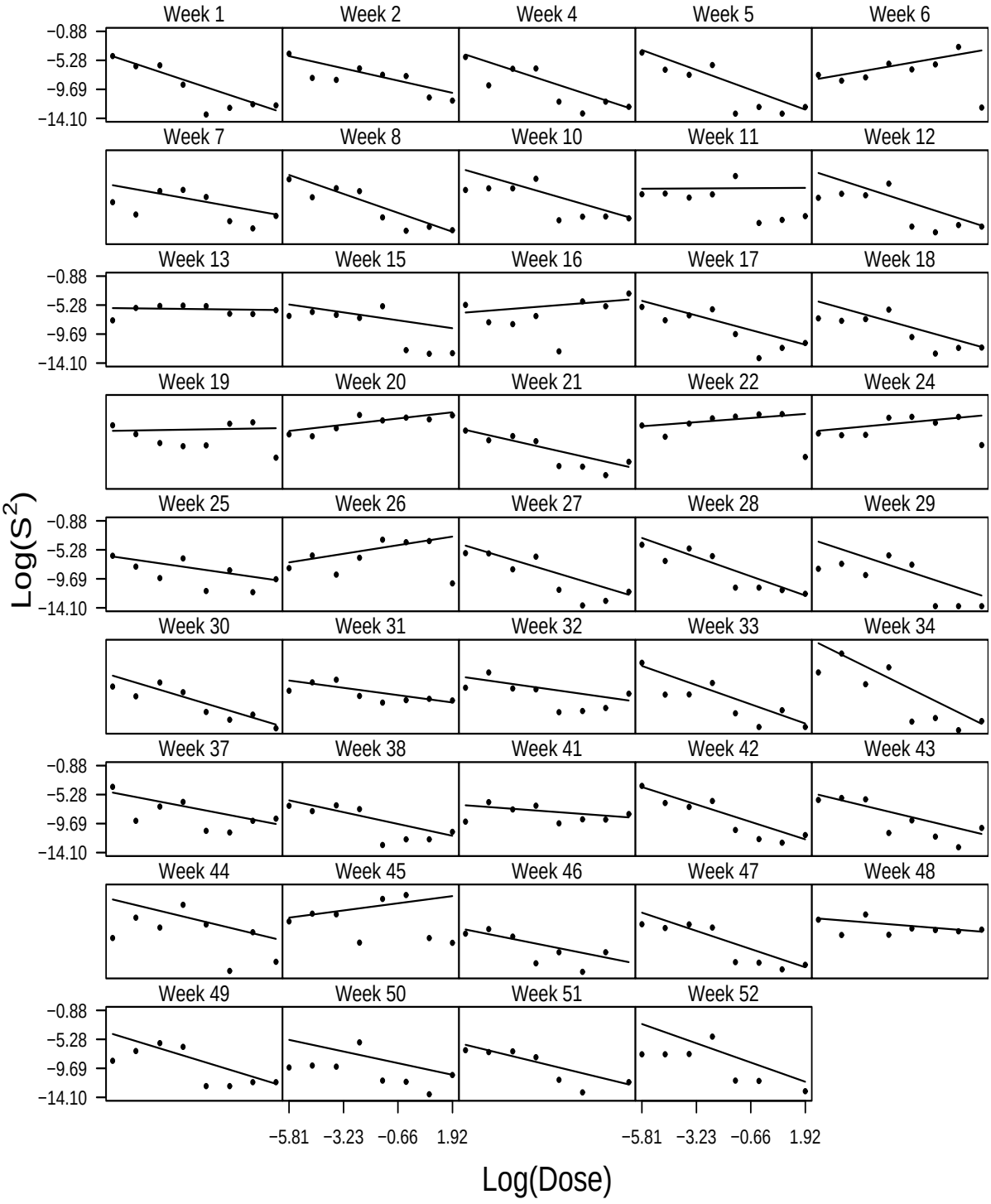

Figure 3: Estimated variance profiles for all 44 weeks, overlaid.

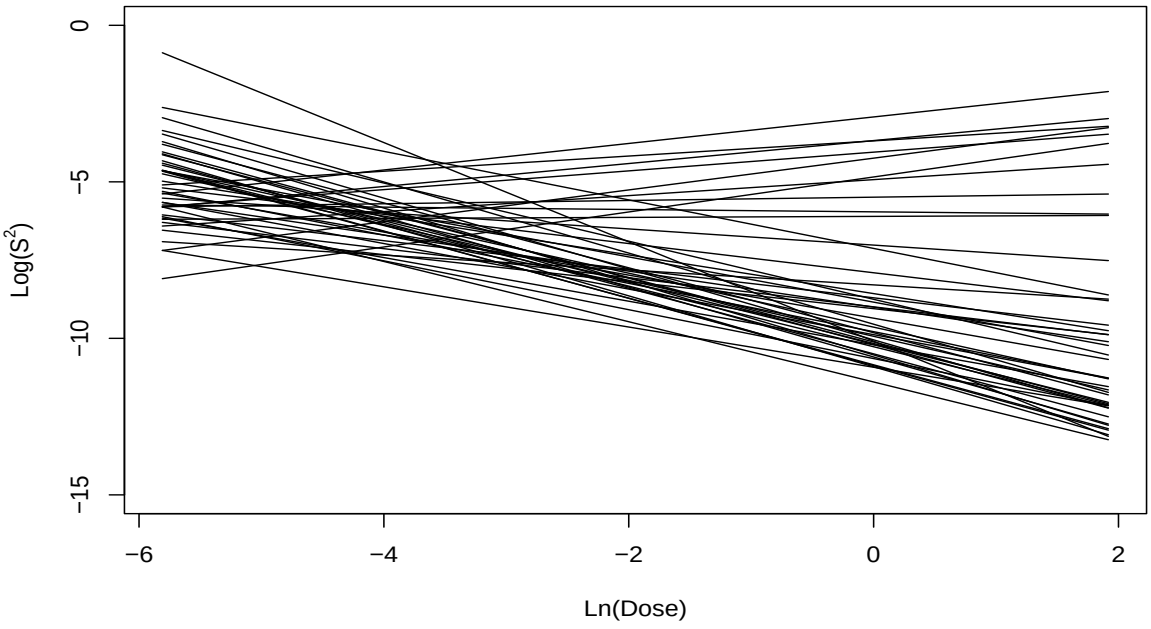

Figure 4: T^2 charts based on (a) $T^2_{MVE,i}$ and (b) $T^2_{D,i}$ to detect unusual variance profiles.

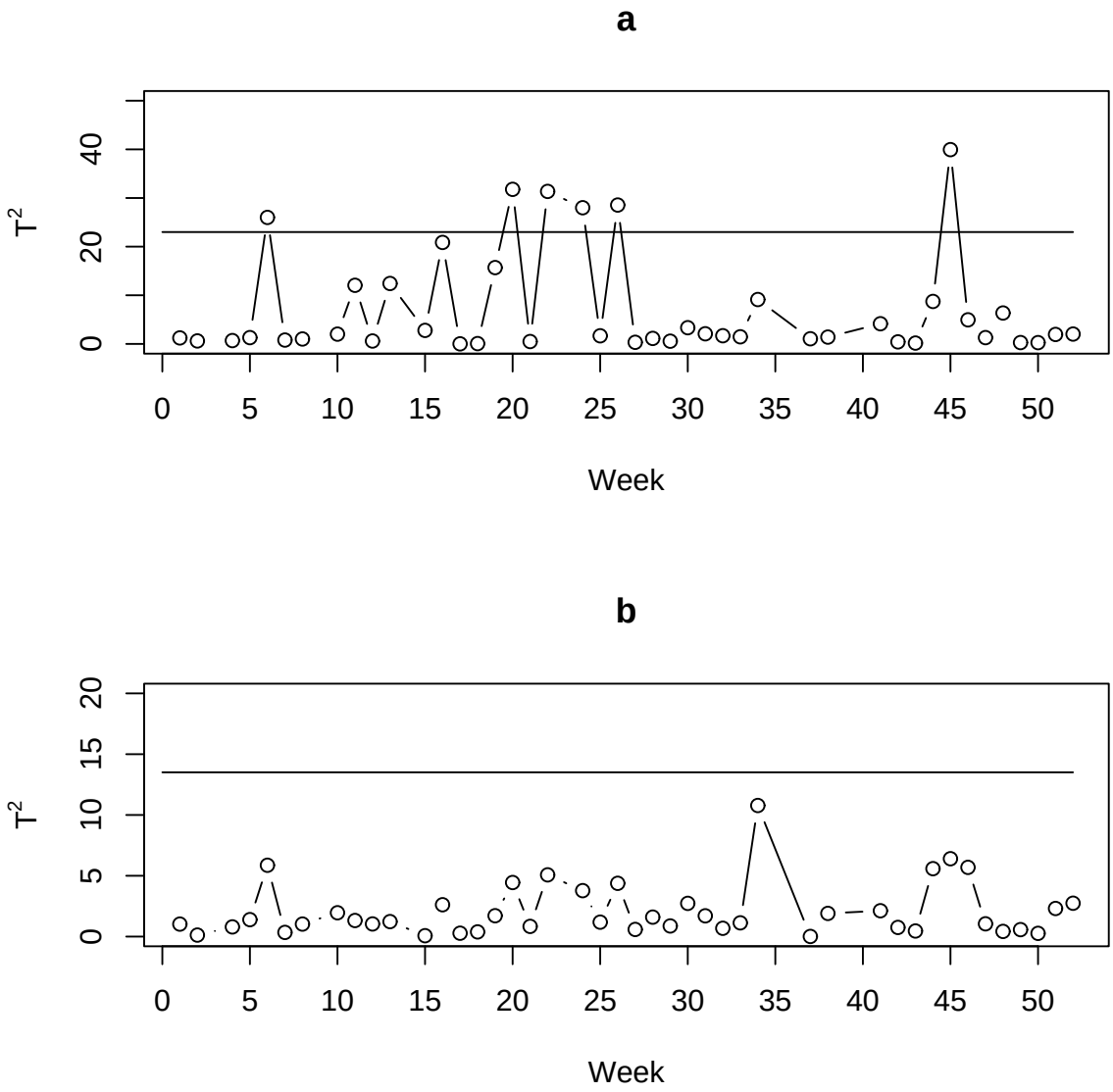

Figure 5: Scatterplot of values of $\hat{\theta}_{0,i}$ and $\hat{\theta}_{1,i}$ for all forty-four weeks of the DuPont HDS. Those six observations that produced a signal in the T^2 chart are indicated with the solid black dot.

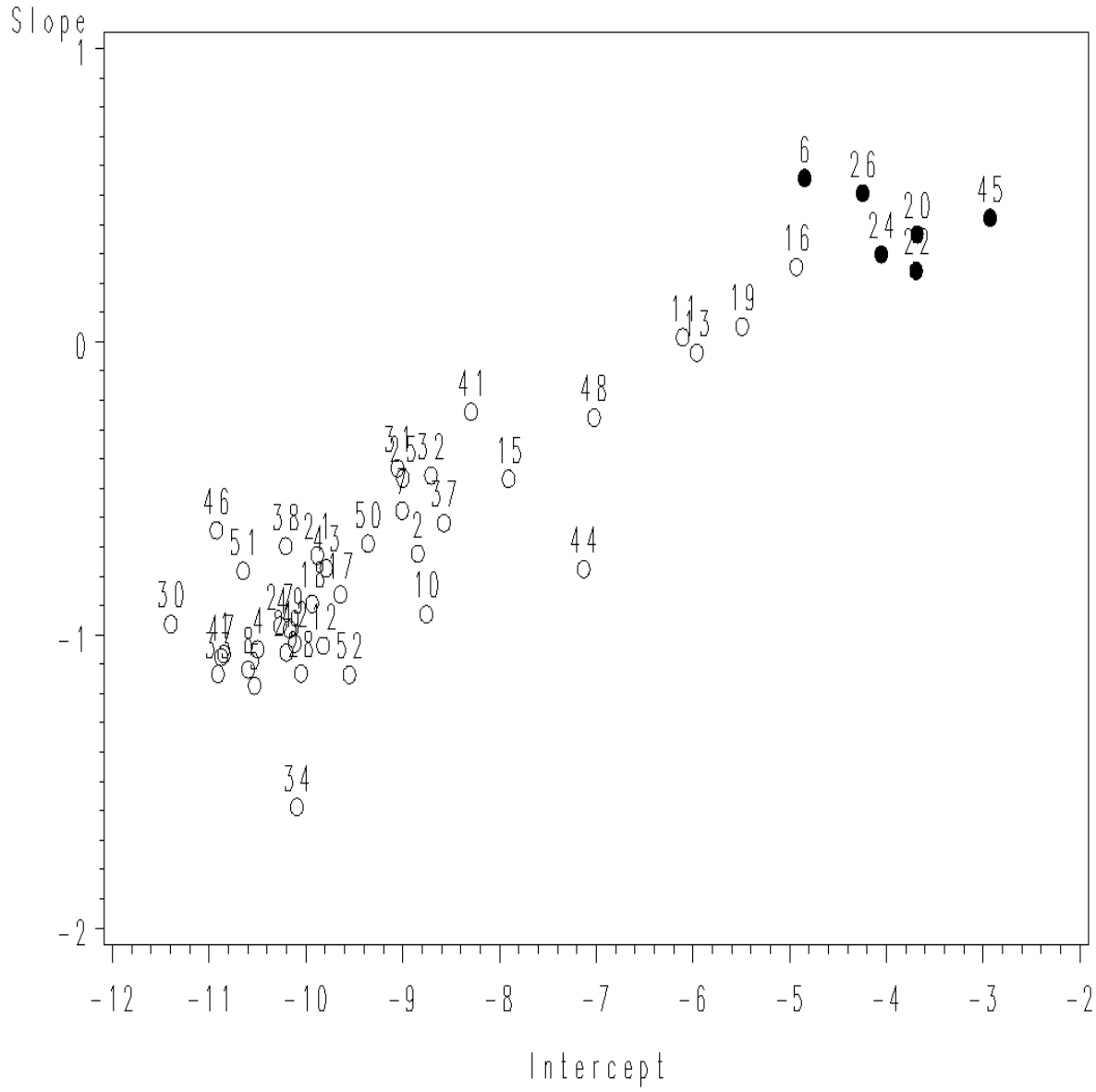

Figure 6: Estimated mean profiles based on estimated weights for all 44 weeks.

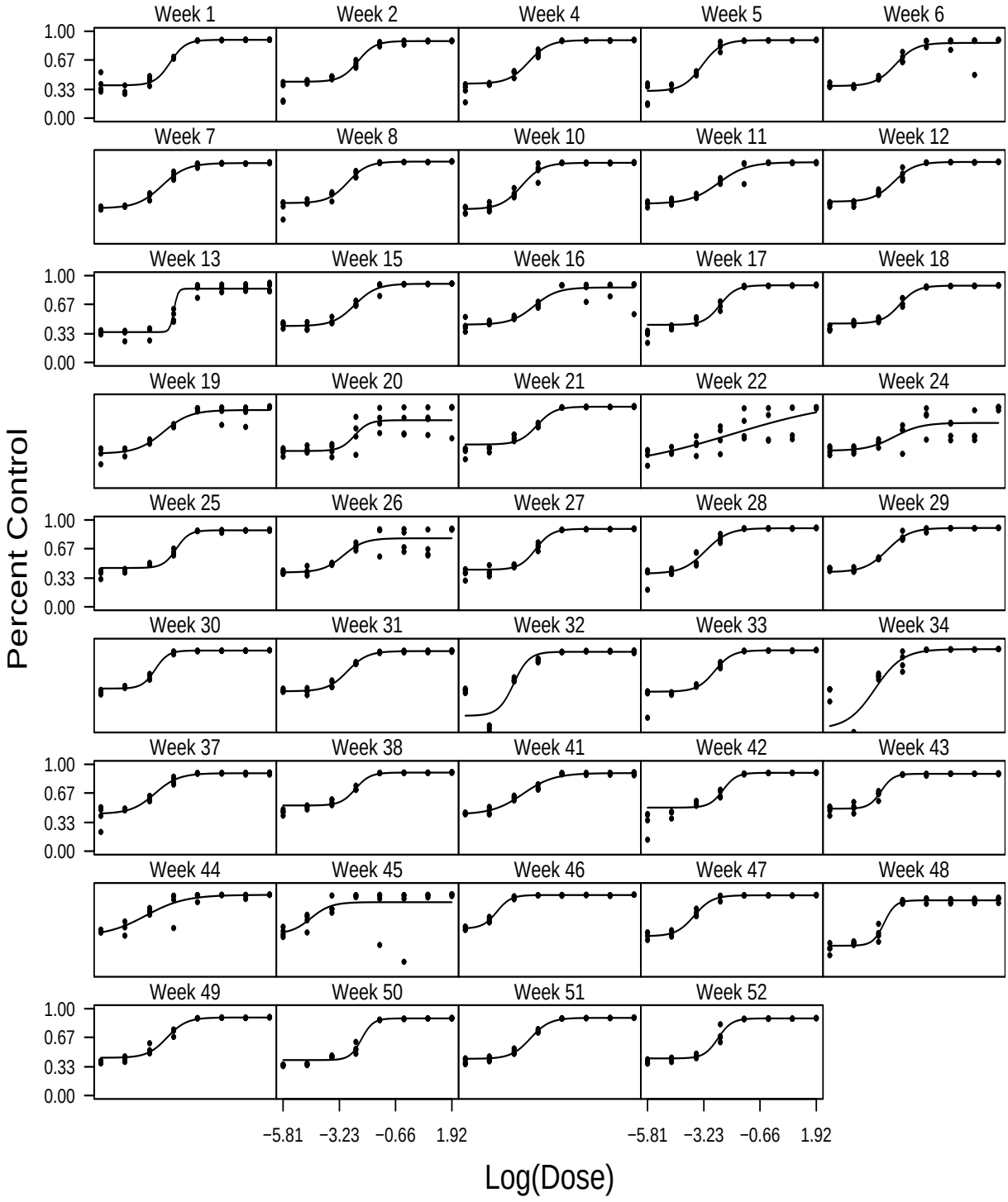

Figure 7: Lack-of-fit chart based on the weighted sums of squares.

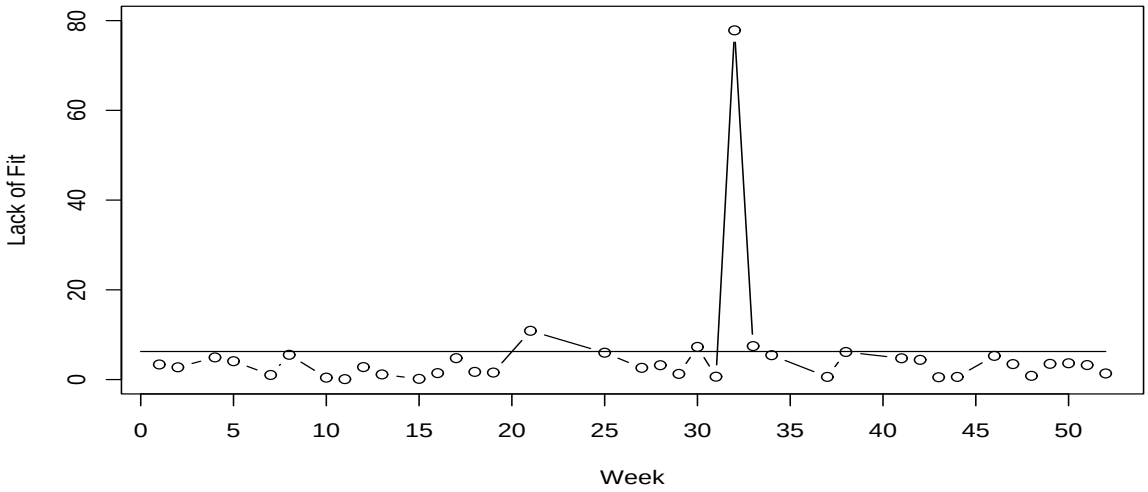

Figure 8: T^2 charts based on (a) $T^2_{MVE,i}$ and (b) $T^2_{D,i}$ to detect unusual values of the parameters estimates of the mean profiles.

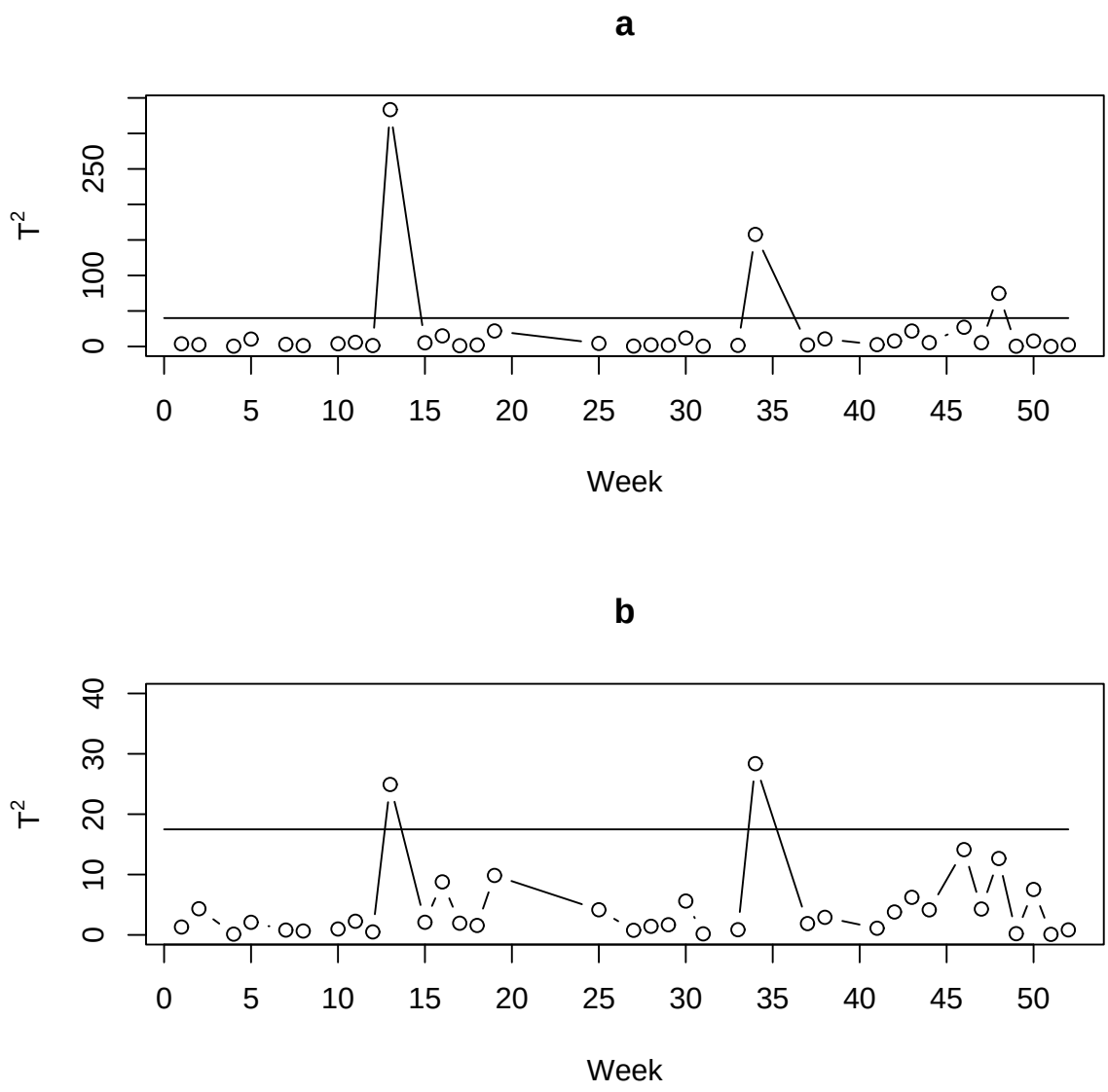

Figure 9: Second set of T^2 charts based on (a) $T^2_{MVE,i}$ and (b) $T^2_{D,i}$ to detect unusual values of the parameters estimates of the mean profiles.

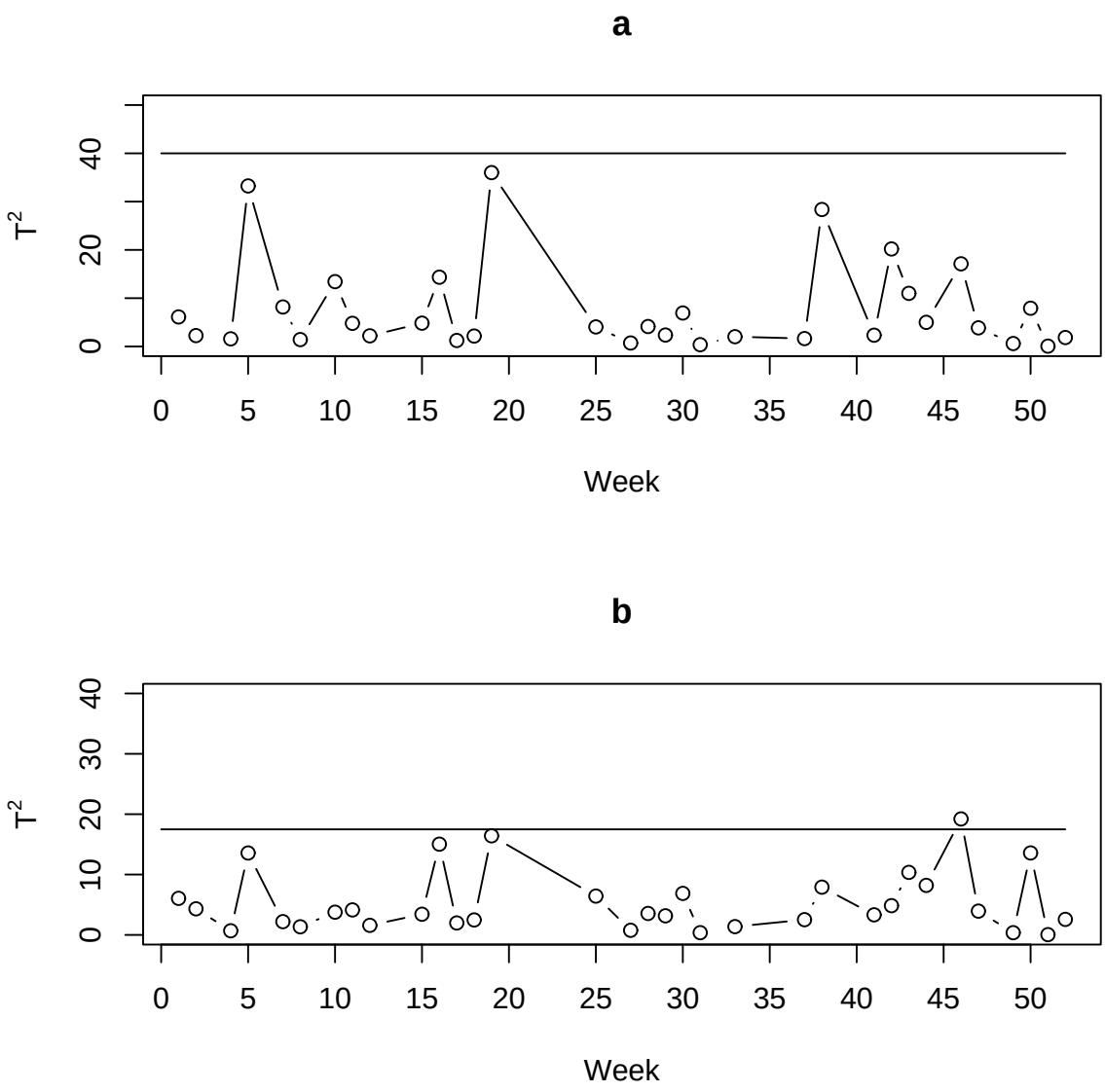

Figure 10: Estimated in-control mean profiles.